Date of publication xxxx 00, 0000, date of current version xxxx 00, 0000.

Digital Object Identifier 10.1109/ACCESS.2017.DOI

Parameter Analysis in Macro-Scale Molecular Communications using Advection-Diffusion

DANIEL TUNÇ MCGUINESS, STAMATIOS GIANNOUKOS, ALAN MARSHALL (Senior Member, IEEE), and STEPHEN TAYLOR

Department of Electrical Engineering and Electronics University of Liverpool Liverpool UK

Corresponding author: Daniel Tunç McGuiness (e-mail: danielmc@liverpool.ac.uk).

The research was funded from the Engineering and Physical Sciences Research Council (EPSRC) under the grant agreement: EP/M029425/1 'Creating a Stink - Investigating Olfactory Transport Streams'

ABSTRACT Molecular communication (MC) is a method where the transmission of information involves the use of chemicals or molecules instead of electromagnetic (EM) waves. The study of MC to date has mostly focused on the nano (nm) to micro (μm) scale and there have been only a few experimental studies on the subject of macro-scale. In this paper properties of macro-scale MC are experimented and studied. These are signal flow (q), carrier flow (Q) and bit duration (T). A mass spectrometer (MS) with a quadrupole mass analyzer is used as the detector and an in-house-built odor generator is used as the chemical pulse generator. The study has shown that the signal energy has a quadratic relation to signal flow whereas the carrier flow has a non-linear relation to both the signal amplitude and the signal energy. The bit duration has shown that the system reaches a saturation point as the bit duration is increased and this effect also occurs in the leftover chemical signal after bit transmission. Finally a mathematical model is developed for the first time to explain the molecular transmission on the macro-scale using advection-diffusion equation.

INDEX TERMS Molecular Communication; Mass Spectrometry; Macro-scale

I. INTRODUCTION

MOLECULAR Communication (MC), i.e. sending information using particles (i.e. molecules) instead of utilizing electromagnetic (EM) waves, has been employed by nature as plant-to-plant communications [1] and by animals (i.e. pheromones [2]–[4]). Recently, this method has seen applications in engineering [5]. However, as this communication can be observed in both very small scales (intercellular, DNA etc.) and large scales (fishes [6], eels [7]), MC is classified into two categories: micro- and macro-scale.

The first study of MC was at conducted in the micro-scale, which can be defined as a system within the transmission distance of nm - μm [8]. One of the drives into the study of micro-scale MC is the difficulty of shrinking an EM antennae into the micro-scale because of constraints such as the antenna size to EM wavelength ratio [8]–[11].

There have been numerous studies in this range of MC, such as transmission using Brownian Motion (MCvD) [12]–[15] and with drift [16]–[19], channel capacity [20]–[25], modulation [26]–[29] and forward error correction [30]. Even though the majority of the studies at this scale have been largely theoretical, there have been applications proposed that utilized micro-scale, e.g., body drug-delivery systems [31], communication between nano-machines [32], machine to neural communications [33].

Using MC at the macro-scale (cm - m) [34], compared to micro-scale, is a relatively new field of study. There have been a few practical [35]–[39] and theoretical [40]–[42] studies, which show that sending chemicals at the macro-scale is possible.

There are applications in which macro-scale communications could be utilized, such as monitoring of infastructure. In [43], it was shown that radio based sensor are not reliable for some application in infastructure monitoring. Because molecular communication is inspired by nature, the knowledge from the understanding of the field can be used a tool for studying biological communications [7], [44], pheremonal communication between robots [45], [46] and odor transmission using digital media [47].

In molecular communications the information can be en-

coded to parameters such as to the release of chemicals [48], [49] quantity (i.e. concentration) [27] and type of chemicals [50]. When the modulated signal is released, it is sent through the medium from the receiver to the detector by a propagation scheme. There are two types of propagation schemes that can be utilized in MC: passive (diffusion) and active (advection-diffusion). However due to the scale of communications (cm - m) it is a better choice to include an active transport mechanism in the communication.

As mentioned, macro-scale MC is a new field with relatively few experimental studies. Some of the fundamental parameters such as the quantity and the advective flow of the system have yet to be studied using experimental methods, in addition to the analysis of these parameters on the properties of the communications such as signal amplitude, energy and SNR.

In [40] a theoretical study was made on the absorption of chemicals based on the Fokker-Plank equation. However in this study the model is based on a variation of the mass transport equation and further developed with experimental data to explain the behaviour of removal of particles (flushing) based on the leftover chemicals present in the detector.

In this study the properties of macro-scale molecular communication are investigated both experimentally and theoretically. These include the signal flow, chemicals that create the signal, carrier flow that help in the transmission of the communication and the bit duration of the pulse. An in-house-built gas generator was used to generate the chemicals pulses and a quadrupole mass analyzer with a triple filter were used. The results show the signal flow affects the signal energy quadratically whereas the carrier flow affects the system in a non-linear way for both the amplitude and the energy of the signal. The bit duration shows that there is a saturation point in the transmission (i.e. the point where the system reaches a steady state) and a mathematical model also show that the overall macro-scale communication can be modelled using a generalized version of the diffusion-advection equation.

In this paper the major contribution is the explanation of the effect of introduction and removal (flush) of the chemicals from the detector by using a derived from of general mass transport equations and comparison to experimental values of the communication parameters such as the signal amplitude, signal energy and signal-to-noise (SNR) ratio to show the validity of the model for use in macro-scale molecular communications.

The rest of the paper is organized as follows. In section II, the experimental setup and each component of it is described in detail. Then in section III the mathematical expression is developed that is used to define the propagation. Sections IV, V and VI are the comparison of experimental results to the theoretical model developed in Section III. The paper ends with concluding remarks with future work in Section VII.

II. EXPERIMENTAL SETUP

In order to test the signal flow (q), carrier flow (Q) and the bit duration (T) of macro-scale MC, two devices were employed. The generation and transmission of chemicals based on a message was made using an in-house-built odor generator, and the detection of the chemical was made with a mass spectrometer (MS) having a quadrupole mass analyzer (QMA). A QMA is an instrument capable of analyzing and distinguishing charged ions or sample molecules by their motion in an applied electric field. The analyzer of the MS allows the detection of ions with a particular mass-to-charge (m/z) ratio [51], [52], making it a useful tool for use in MC. The diagram for the experimental setup used in the study can be seen in Figure 1.

A. TRANSMITTER

A gas dispenser that is controlled by mass flow controllers (MFC's) releases volatile organic compounds (VOC) (placed into an evaporation chamber) called the signal flow (in this experiment the signal flow is chosen as acetone), whereas the flow passing through the mixing chamber is called the carrier flow (N_2) [37], [53].

VOCs are chemicals that can transmit from the liquid to the gas phase at ordinary room temperature and pressure. This property is caused by the low boiling point of the chemical, which forces large number of molecules to evaporate from its liquid or sublimate from its solid phase and mix-in with the surrounding air, known as volatility. Most odors are comprised by VOCs.

The MFC's are connected directly into the N_2 gas cylinder and controlled directly by a computer and an automation platform. The automation platform sends digital commands to the MFC and the internal valve inside can be controlled to create gas pulses. In this setup, there are two flows present; one is responsible for transporting the samples from the evaporation chamber into the mixing chamber (signal flow q). The second one is responsible for carrying the signal chemicals from the mixing chamber to the transmission medium (carrier flow Q). The diagram for odour gas generator can be seen in Figure 2 and the evaporation chamber can be seen in Figure 3. When the gas leaves the mixing chamber and transmits through the medium it is defined as bulk flow (B) [37], [53].

$$B = Q + q \tag{1}$$

B. CHEMICALS

In these experiments three types of chemicals were employed. A Zero-grade N_2 (% 99.998 purity) was chosen for the carrier gas (Q) that carries both the signal chemical from the transmitter to the detector and transports the signal chemical from the evaporation chamber to the transmitter. The signal gas (q) was chosen as acetone (% 99.8 purity, CAS Number: 67-64-1), which was both diluted in methanol (over % 99.9 purity). The dilution in methanol produced a $\approx$ % 9 solution of concentration of the sample (1-part acetone, 10-part methanol). Both acetone and methanol were introduced to the system in its liquid phase. and N_2 was stored in its gas phase.

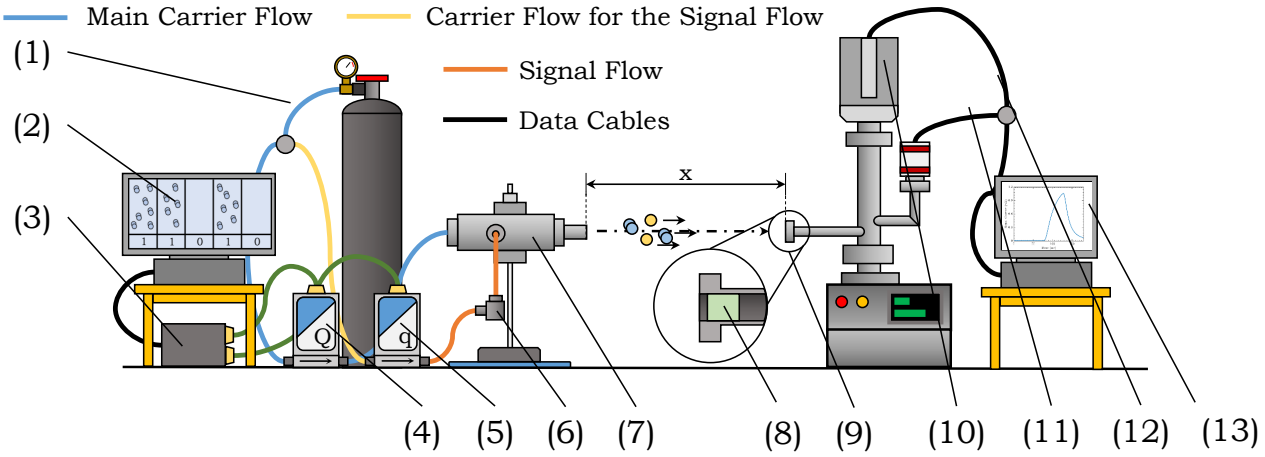

FIGURE 1: The diagram of the experimental setup: **(1)** (N_2) gas is used as the carrier flow (Q) and is transferred into the MFC that control both the carrier flow (blue line) (Q) and the signal flow (yellow line) (q) **(2)** Modulation information is generated using a computer software **(3)** generated modulation is transmitted into an automation platform where it sends the modulation to the MFC's to create pulses **(4)** MFC for the carrier flow **(5)** MFC for the signal flow **(5)** Evaporation Chamber (EC) where the signal chemical is injected **(7)** Mixing chamber where the signal chemicals arrive and initiate the transmission from the transmitter to the detector **(8)** Semipermeable membrane present in the inlet of the mass spectrometer **(9)** the inlet of the mass spectrometer **(10)** electronics control unit (ECU) which controls the mass analyser **(11)** Pressure gauge **(12)** Controller and the requlator cables for the mass spectrometer **(13)** Data acquisition and analysis

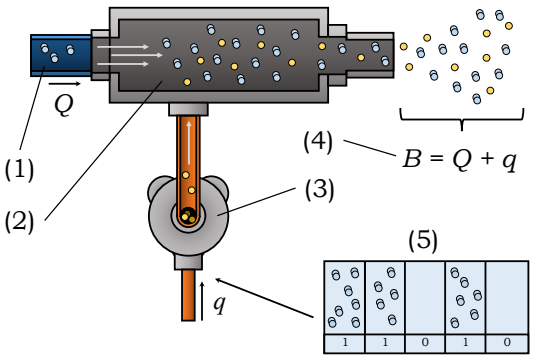

FIGURE 2: The working diagram of the gas generator [53] **(1)** Introduction of the carrier gas (Q) into the mixing chamber **(2)** Mixing chamber where the evaporated chemicals from the chamber and the carrier gas are mixed **(3)** evaporation chamber (Figure 3) **(4)** Transmitted chemicals that are released from the chamber. **(5)** A modulation sequence that is used to create gas pulses

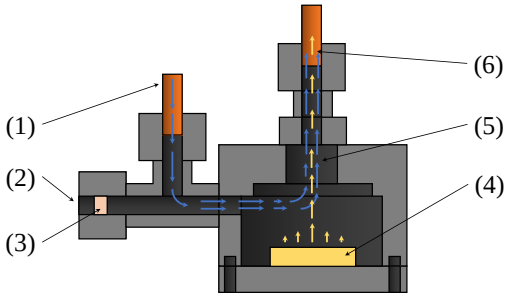

FIGURE 3: Diagram of the evaporation chamber: **(1)** Inlet of the N_2 gas into the evaporation chamber **(2)** Inlet where the sample is introduced **(3)** thermo-resistant septum that lets multiple introduction of a sample introduction via a micro syringe **(4)** An absorptive material that holds the liquid sample analyte **(5)** N_2 from the inlet carries the evaporated chemicals from the chamber **(6)** The cumulated gas it transferred into the mixing chamber via a 0.25 inch Teflon tube.

C. DETECTOR

A portable membrane inlet mass spectrometer (MIMS), provided by Q Technologies Ltd., was used as the primary sensor for detecting the transmitted chemicals. The applications and the properties of the MIMS are described in the literature [54]–[59].

A MIMS consists of three primary parts: a sampling probe that lets the gas sample to pass membrane for the MS to analyze, A triple filter quadrupole mass spectrometer (QMS, which in turn consists of an electron ionization source (EI), mass analyzer and a detector and finally a vacuum system. with the inlet of the system having a fine non-sterile flat polydimethylsiloxane membrane [37], [57]. Additional details about the detector and the overall design of the system can be found in [37].

Chemical introduction into the system is done through a non-sterile flat polydimethylsiloxane (PDMS) membrane. Due to the presence of the membrane, each chemical can have a different arrival time and because each chemical can interact with the membrane differently, each chemical can have a different absorption rate [37]. The details of the membrane and its applications can be seen in [57].

In this study, parameters of macro-scale molecular communications are experimented. These a parameters are as follows; signal flow (q), carrier flow (Q) and the bit duration (T). All experiments are conducted in open-air where the is no boundary (i.e. pipe) between the transmitter and the detector and the distance between is x = 2.5 cm.

In the following section a mathematical model is developed to explain the signal pulses of a molecular communication system.

III. TRANSMISSION OF MOLECULES

A communication based on the transmission of particles (i.e molecules, silt, pollutants etc.) can be explained using the mass transport phenomena. This can be briefly explained as the exchange of mass, energy, charge and momentum between observed systems. Since molecular communications utilizes the mass of the particles in the exchange between systems, Fick's 2nd law can be used to describe the system when there is no flow present in the system [60].

$$\frac{\partial C}{\partial t} = D\nabla^2 C \tag{2}$$

At micro scales (nm - μm) the above equation can be used to model and explain the whole system. However at macro-scales (cm - m) the system needs external propulsion to transmit the chemicals. Therefore an additional parameter, the advection flux, is needed to introduce the flow component into the system. To describe the system, a generalized expression of advection-diffusion (general scalar transport [61]) equation is used.

$$\frac{\partial C}{\partial t} = D\nabla^2 C - \nabla \cdot (\mathbf{u}C) + R \tag{3}$$

To simplify the equation, it is assumed that the diffusion coefficient (D) is constant, there are no sources or sinks (R = 0), and the velocity has zero divergence. Based on these the equation can be rewritten as

$$\frac{\partial C}{\partial t} = D\nabla^2 C - \nabla \cdot (\mathbf{u}C) \tag{4}$$

The solution for the partial differential equation with an instantaneous (t = 0) and localized (x = 0 , y = 0, z = 0) for 1D, 2D and 3D releases are as follows

$$C(x,t) = \frac{M}{A_{yz}\sqrt{4\pi D_x t}} \exp\left(-\frac{\eta_x^2}{4D_x t}\right) \tag{5}$$

$$C(x,y,t) = \frac{M}{L_z 4\pi t\sqrt{D_x D_y}} \exp\left(-\frac{\eta_x^2}{4D_x t} - \frac{\eta_y^2}{4D_y t}\right) \tag{6}$$

$$C(x,y,z,t) = \frac{M}{(4\pi t)^{3/2}\sqrt{D_x D_y D_z}} \exp\left(-\frac{\eta_x^2}{4D_x t} - \frac{\eta_y^2}{4D_y t} - \frac{\eta_z^2}{4D_z t}\right) \tag{7}$$

Where M is the mass introduced into the system (kg), D_x, D_y and D_z are the diffusive coefficients in x, y and z coordinates respectively (cm^2/s) A_{yz} and L_z are the area-scale and length-scale of the neglected dimensions. t is the duration of the experiment (s), C is the concentration of the chemical in 1D, 2D and 3D (kg/m, kg/m^2 and kg/m^3) and η_x, η_y and η_z are the moving reference frames with the following descriptions. In macro-molecular communications, the diffusion (D_x, D_y and D_z) caused by the particles may be governed by a combination of momentum and turbulent diffusion.

$$\eta_x = x - (x_0 + u_x t) \tag{8}$$

$$\eta_y = y - (y_0 + u_y t) \tag{9}$$

$$\eta_z = z - (z_0 + u_z t) \tag{10}$$

Where x_0, y_o and z_o are the injection points of the mass, u_x , u_y and u_z are the mean flow velocity and $u_x t$, $u_y t$ and $u_z t$ are the distances the centre of mass of the cloud travelled in a given time of t.

To model the molecular transmission, the detector is assumed ideal (i.e. when absorbed the particles are not released and given enough time the detector will have absorbed all the particles in the system) and the injection point of the chemical is measured as x_0 = 0. The visual representation of the model can be seen in Figure 4. For a bit duration of T, the particle concentration of the bit value of 1 in 1D can be expressed as

$$C_1(x,t) = \frac{M}{\sqrt{4\pi D_x t}} \exp\left(-\frac{\eta_x^2}{4D_x t}\right) \quad 0 \le t \le T \tag{11}$$

Therefore the the particles that are absorbed by the detector can be shown as

$$\theta_c(x,t) = M - \int_{-x_\epsilon}^{x_d} \frac{M}{A_{yz}\sqrt{4\pi D_x t}} \exp\left(-\frac{\eta_x^2}{4D_x t}\right) dx \tag{12}$$

$$\theta_c(x,t) = M - \frac{M}{2A_{yz}} \left[\text{erf}\left(\frac{x_d - u_x t}{2\sqrt{D_x t}}\right) + \text{erf}\left(\frac{x_\epsilon + u_x t}{2\sqrt{D_x t}}\right)\right] \tag{13}$$

$$\int_{-\infty}^{+\infty} C(x,t)dx = M \tag{14}$$

When the duration the transmission has ended for bit 1, the system will introduce the flush concentration to the system. This will counteract the particles present in the detector and start to deplete the chemicals from the detector. However, since the time it takes for the detector to absorb all the chemicals in the system can take longer than the duration of the bit, the particles that have been absorbed by the detector should be calculated which can be less than the particles released from the transmitter. Therefore particle in the detector can be calculated as

$$M_R = \theta_c(x,T) - \theta_c(x,0) \tag{15}$$

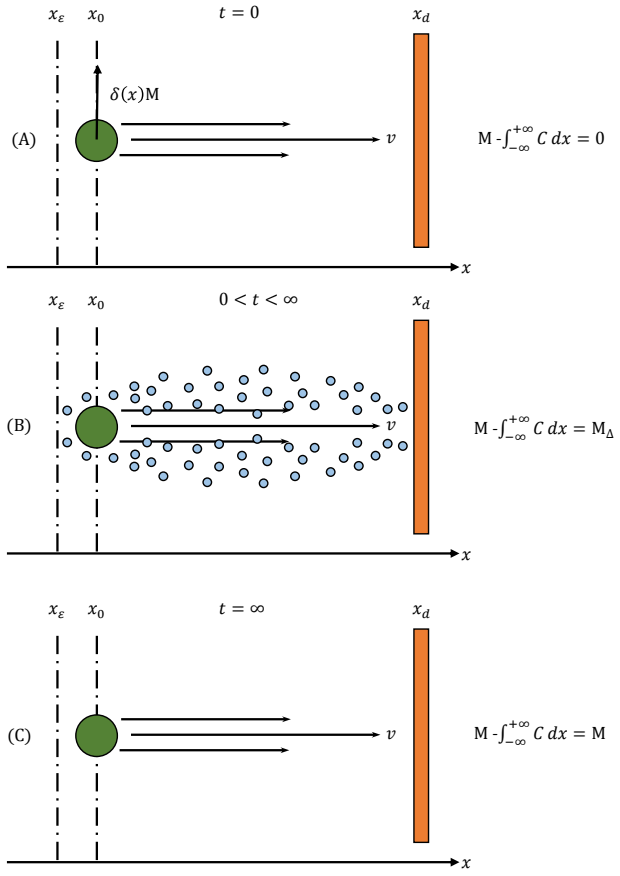

FIGURE 4: A visual description of the boundaries and the conditions of the model: (A) At the beginning of the transmission (t = 0) chemicals are released into the system instantaneously. This is described as a Dirac function (B) As the system evolves the chemicals stars to propagate to the detector, however due to the diffusive nature of particles, some particles will propagate against the detector (C) After enough time has passed the detector will have absorbed all the chemicals in the system

The concentration that produces the flush (bit 0) part of the transmission can be written as.

$$\theta_{c_0}(x,t) = \frac{M_R}{2A_{yz}}\left[\mathrm{erf}\left(\frac{x_d - u_x t}{2\sqrt{D_x t}}\right) + \mathrm{erf}\left(\frac{x_\epsilon + u_x t}{2\sqrt{D_x t}}\right)\right] \tag{16}$$

In this method of transmission, a measure of which part is dominant (advection or diffusion) can be estimated by using a dimensionless parameter called a Péclet Number. This is defined as

$$\mathrm{P}\acute{e} = L\frac{u}{D} \tag{17}$$

For systems with P$\acute{e} \ll 1$, the diffusion property dominates the system and for P$\acute{e} \gg 1$, the advection (flow) dominates. Based on Eq. (17) it can be inferred that as the transmission evolves and the transmission distance increases, the system will eventually become advection based and diffusion will play a lesser part in macro-scale molecular communications with a flow present in the system.

TABLE 1: Experimental Parameters for Signal Flow Experiment

Parameter	Symbol	Value	Unit
Tracked signal flow ion	m/z	43	Da
Carrier flow	Q	750	ml/min
Bit Duration	t_{bit}	300	s
Transmission distance	x	2.5	cm
Carrier flow pressure	P_F	1	bar
Diffusivity of acetone in air	D	0.124	cm^2/s

IV. SIGNAL FLOW

Signal flow (q), in the system, is defined as the concentration value of the chemical that is used in the transmission of information. As a way of introducing the chemicals to the system, this property of the transmission can be correlated to the M parameter of the equation given in Eq. (5) in Section II. However, unlike the M parameter which describes a mass, in the experiment M consists of volatile organic compounds (VOCs) in gas form. In addition since this property in the experimental setup is by nature flow, and not a direct injection of particles, the M parameter can change if the carrier flow (Q) property is varied which will be discussed in Section V.

In the setup, mentioned in Section II, this property is controlled by using mass flow controllers (MFC's) and an automation platform. An experiment was conducted to test the communication properties of the signal flow (q) for molecular communications and the parameters for the experiment are given in Table 1.

A. SIGNAL PROPERTIES

The results for the signal flow transmission experiments can be seen in Figure 5 and 6. As it can be seen, the signal increases in amplitude and the relation between these parameters is linear as seen in Figures 5 and 6. However, the increase of signal creates increased distortion which can be observed in Figure 5. Therefore the effect the variance (σ^2) of the signal when signal flow is varied is measured. The variance is calculated as

$$V = \frac{1}{N-1}\sum_{i=1}^{N} \mid A_i - \frac{1}{N}\sum_{i=1}^{N} A_i \mid \tag{18}$$

Based on the experimental results, the variance of the signal with respect to the signal flow (q) can be seen in Figure 7 (a) and can be approximated as

$$\sigma^2 \approx 0.001q^2 \tag{19}$$

This is due to the fact that as the signal flow (q) increases, the chemicals present in the system increase as well, which increases the number of particles diffused in a way that is detrimental to the transmitted signal.

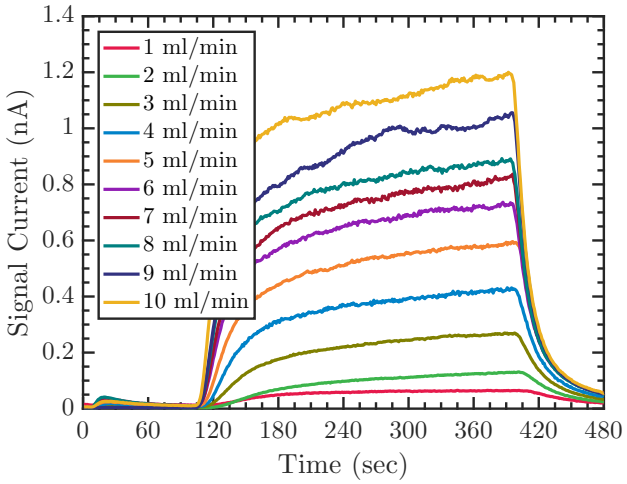

FIGURE 5: Experimental results of the signal flow transmission experiment where signal flow is q = 1 ml/min to 10 ml/min with 1 ml/min increments

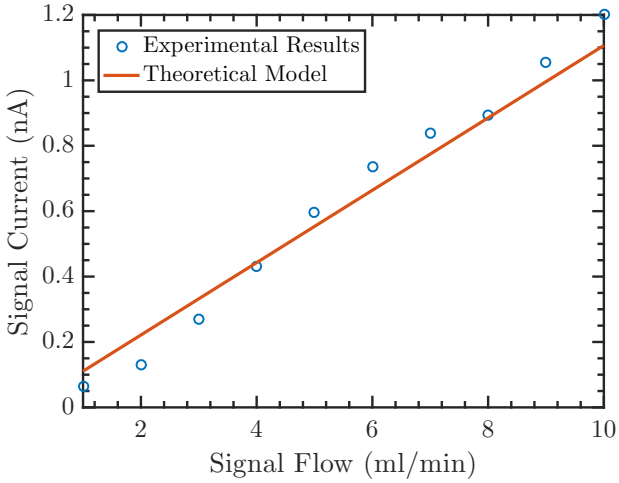

FIGURE 6: Experimental results of the maximum amplitude generated where signal flow is q = 1 ml/min to 10 ml/min with 1 ml/min increments (M = 0.112 ngr, D = 0.05 cm^2/s, u = 0.05 cm/s, x = 2.5 cm) (R^2 = 0.99)

To calculate the signal correlation between two signals the Pearson correlation coefficient is used. The equation of the coefficient is given below.

$$\rho_{X,Y} = \frac{\text{cov}(X,Y)}{\sigma_X \sigma_Y} \tag{20}$$

The result can be seen in Figure 7 (b). As it can be seen the signal quantity increase has a negative effect on the correlation to the original signal (q = 1 ml/min). This is caused by the diffusion of particles which in turn is caused by increased introduction of chemicals into the system.

B. SIGNAL ENERGY AND SNR

When a sample is to be analyzed by a MS, the sample is ionized and detected by a detector. In our system the detector produces current (I) from the introduction of the samples (θ).

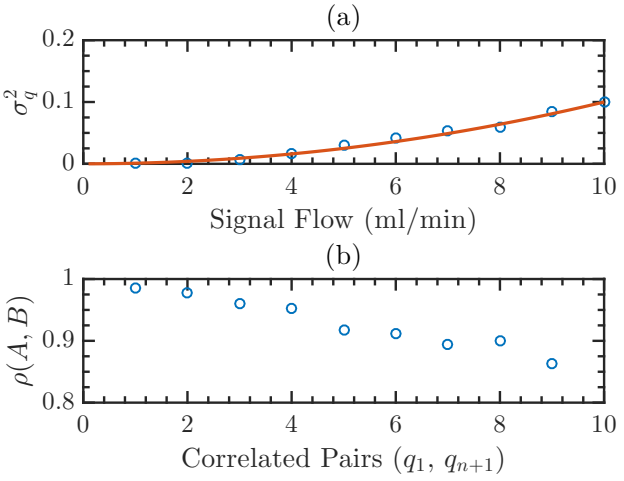

FIGURE 7: (a) Experimental result of the signal variance (σ^2) as the signal flow (q) is increased (R^2 = 0.99) (a = 0.01) (b = 2) (b) Signal correlation of pairs from the signal flow experiment

Therefore, the energy of a continuous signal (ϕ_C), can be calculated using

$$\phi_c(x,t) = \int_{-\infty}^{+\infty} |\, \theta_c(x,t)\,|^2\, dt \tag{21}$$

$$\phi_c(x,t) = \int_{-\infty}^{+\infty} \Bigg| M - \frac{M}{2A_{yz}} \left[\text{erf}\left(\frac{x_d - u_x t}{2\sqrt{D_x t}}\right) + \text{erf}\left(\frac{x_\epsilon + u_x t}{2\sqrt{D_x t}}\right)\right] \Bigg|^2 dt \tag{22}$$

$$\phi_c(x,t) = M^2 \int_{-\infty}^{+\infty} \Bigg| 1 - \frac{1}{2A_{yz}} \left[\text{erf}\left(\frac{x_d - u_x t}{2\sqrt{D_x t}}\right) + \text{erf}\left(\frac{x_\epsilon + u_x t}{2\sqrt{D_x t}}\right)\right] \Bigg|^2 dt \tag{23}$$

Based on Eq. (23), it can be seen that the signal flow parameter (M) has a quadratic relation to the energy the signal produces. However due to the presence of error functions in the equation, the comparison of experimental results to derived data was done numerically, which can be seen in Figure 8.

To calculate the signal-to-noise ratio of the system the following equation is used.

$$SNR_{dB} = 10 \log_{10}\left(\frac{\phi_c}{N}\right) \tag{24}$$

Where N is the power of the noise. In the experiment, the noise is analysed experimentally by calculating the variance of the noise (σ_N^2) and modelled as Additive White Gaussian Noise (AWGN) with the following mathematical expression.

$$N = \mathcal{N}(\mu_N, \sigma_N^2) \tag{25}$$

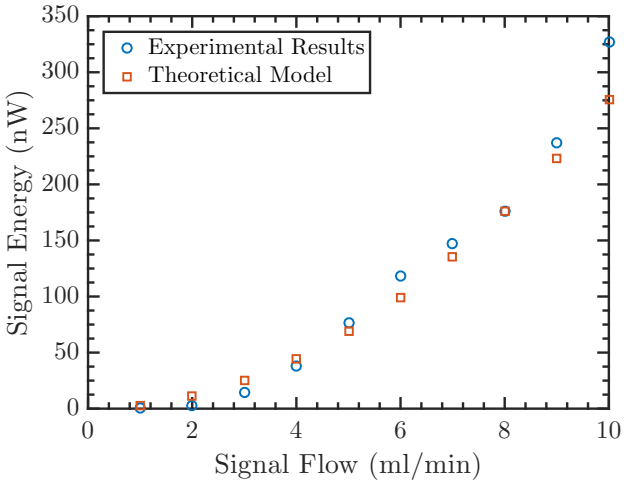

FIGURE 8: Experimental Results of the signal energy values obtained from the signal flow study compared to the numerical results of the theoretical model (M = 0.112 ng, D = 0.05 cm^2/s, u = 0.05 cm/s, x = 2.5 cm) (R^2 = 0.99)

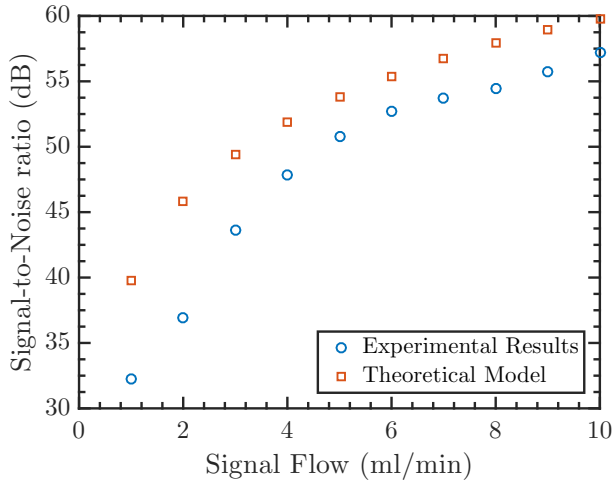

FIGURE 9: Experimental Results of the signal-to-noise values obtained from the signal flow study compared to the numerical results of the theoretical model (M = 0.112 ng, D = 0.05 cm^2/s, u = 0.05 cm/s, x = 2.5 cm, N = 2.8655e-4) (R^2 = 0.98)

The results for the SNR value comparison can be seen in Figure 9.

C. MODELLING OF THE SIGNAL

To test the validity of the model described in Section II, three values of the signal flow experiment (q = 3 ml/min, 6 ml/min and 9 ml/min) were compared to the results obtained from theory. The result of this comparison can be seen in Figure 10. As it can be seen the model shows agreement with the experimental results. However, it should be pointed out that the chemical that are 'flushed' out of the system occur in a faster rate than the model would normally predict. However, by introducing a parameter to the flush velocity, the model's values approaches to the experimental results. This

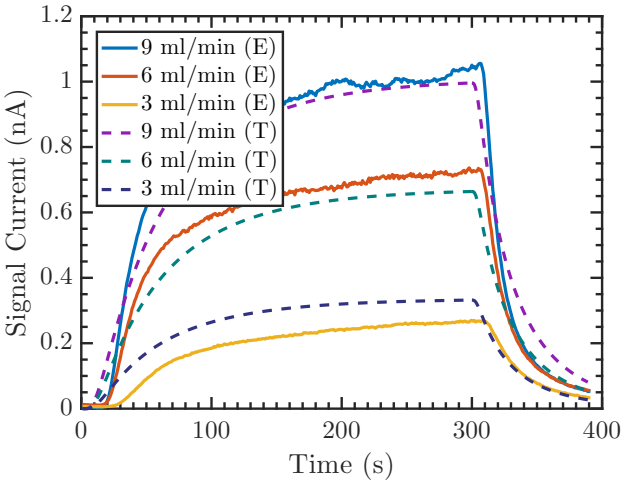

FIGURE 10: Three of the experimental results (q = 3 ml/min, 6 ml/min and 9 ml/min) compared to the theoretical model. (E) experimental results (T) Theoretical model

TABLE 2: Experimental Parameters for Carrier Flow Experiment

Parameter	Symbol	Value	Unit
Tracked signal flow ion	m/z	43	Da
Signal flow	q	8	ml/min
Bit Duration	t_{bit}	300	s
Carrier flow pressure	P_F	1	bar
Transmission distance	x	2.5	cm
Diffusivity of acetone in air	D	0.124	cm^2/s

effects occurrence can be caused by the membrane in the inlet sampling probe of the detector.

V. CARRIER FLOW

Carrier flow can be defined as the flow which aids the transmission from the transmitter to the receiver. The flow decreases the amount of time needed to travel the distance thereby increasing the transmission speed, however the introduction of a carrier flow decreases the concentration of the signal flow which decreases the amplitude of the signal. An experiment was conducted to test the communication properties of the carrier flow (Q) for molecular communications and the parameters for the experiment are given in Table 2.

A. PROPERTIES OF THE SIGNAL

The results of the signal flow transmission experiments can be seen in Figure 11 and the maximum amplitude values of each transmission can be seen in Figure 12. As it can be seen, the signal sees a decrease in amplitude as the flow velocity is increased. This is due to the desaturation of the signal chemicals that are transmitted. This effect occurs because of the way chemicals are transmitted in the experimental setup. Increased carrier flow decreases the amount of chemicals that are transmitted from the mixing chamber to the transmission

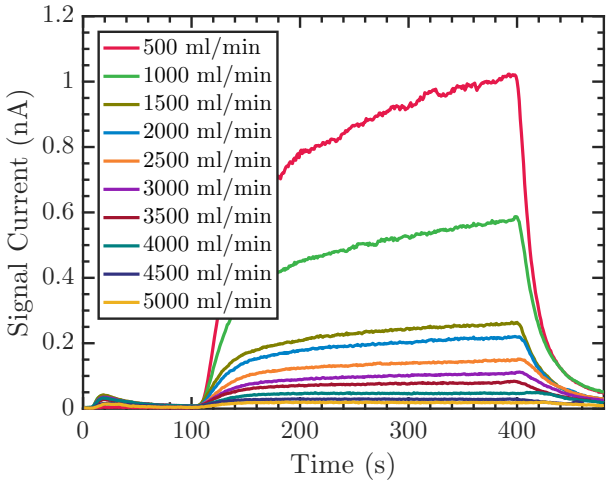

FIGURE 11: Experimental results of the carrier flow transmission experiment where carrier flow is Q = 500 ml/min to 5000 ml/min with 250 ml/min increments

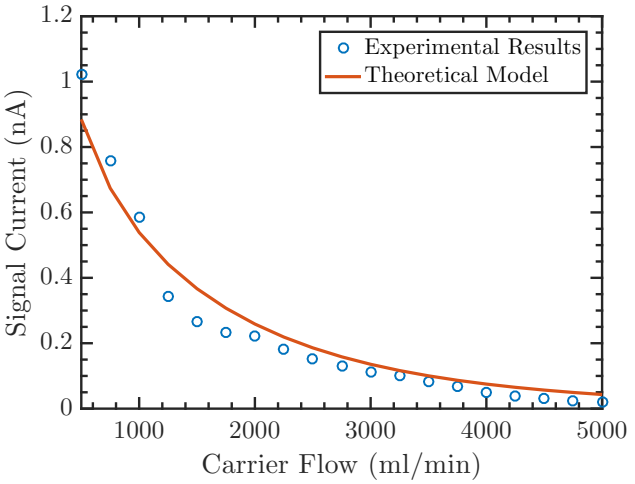

FIGURE 12: Experimental results of the maximum amplitude generated where carrier flow is Q = 500 ml/min to 5000 ml/min with 250 ml/min increments (M = 0.8 ng, D = 0.35 cm^2/s, x = 2.5 cm) (R^2 = 0.97)

medium. As the carrier flow is increased the pressure in the mixing chamber increases as well, which in turn causes a negative effect on the introduction of the signal flow into the evaporation chamber (EC). This effect can be approximated by the following equation.

$$M_n = ME_1\left(\frac{vx}{D}\right) \tag{26}$$

Where E_1 is the exponential integral. By introducing the equation into the calculation the new mass can be calculated. Based on this, it can be seen in Figure 12 that the model shows an agreement to the experimental results.

As the flow value increases, the shape of the signal becomes similar to that of a square wave.This behaviour can be explained by taking the limit of the absorbed concentration function $\theta_C(x,t)$.

$$\lim_{v\to\infty} \theta(x,t) = M \tag{27}$$

This is because the dominance of the flow (advection) rises and the effect of random movements (i.e. diffusion) becomes less apparent. This effect can be also seen in the variance (σ^2) of the signal in Figure 13 (a). The decrease in signal correlation can also be observed in Figure 13 (b), however unlike the signal flow where diffusion plays a role, in carrier flow the decorrelation is caused by the lack of particles in the system and the signal level approaching to the background noise of the detector.

B. SIGNAL ENERGY AND SNR

The signal energy for the carrier flow experiment can be calculated from Eq. (23). As mentioned in the signal flow experiment numerical results are calculated and used for comparison to experimental data. The results can be seen in Figure 14 for signal energy and in Figure 15 for SNR values.

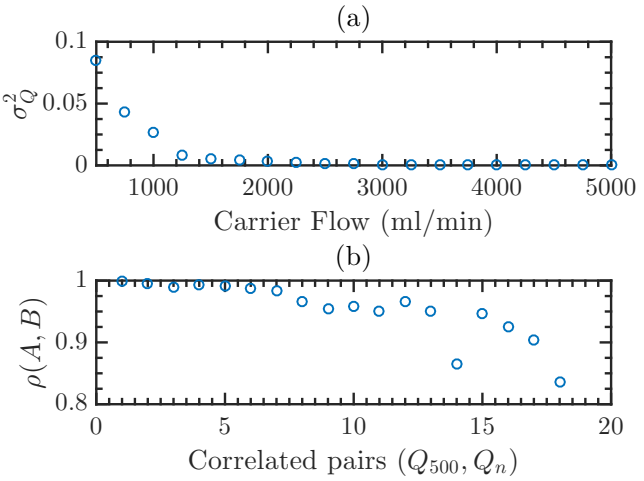

FIGURE 13: (a) Experimental result of the signal variance (σ^2) as the carrier flow (Q) is increased (b) Signal correlation of pairs from the carrier flow experiment

C. MODELLING OF THE SIGNAL

In Figure 16 the comparison of an experimental signals (E) to the modelled signals (T) are shown. As it can be seen, the model is able to predict the signal in lower flow values however as the flow is increased the model diverges from the experimental data.

VI. TRANSMITTED BIT DURATION

Transmitted bit duration (T) is briefly explained as the time each bit is given. Depending on the duration given, different properties of the communication system might occur. One of the properties and a problem for MC is the leftover chemicals influencing the next bit. This effect, known as Inter-symbol Interference (ISI), is a problem that limits the throughput of the system. The parameters for the experiment are given in

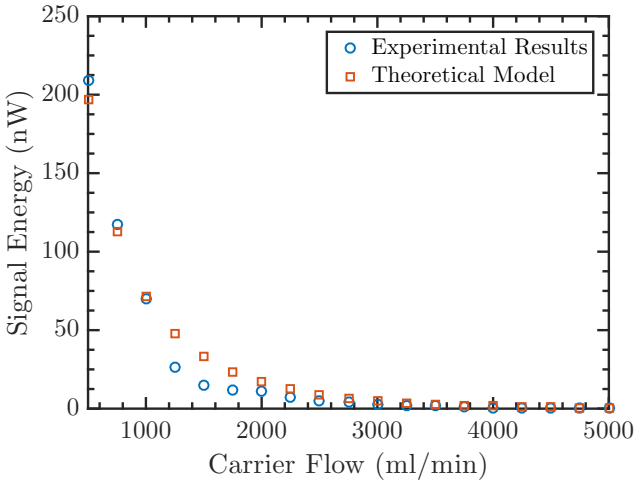

FIGURE 14: Experimental Results of the signal energy values obtained from the carrier flow (Q) study compared to the numerical results of the theoretical model (M = 0.8 ng, D = 0.35 cm^2/s, x = 2.5 cm) (R^2 = 0.98)

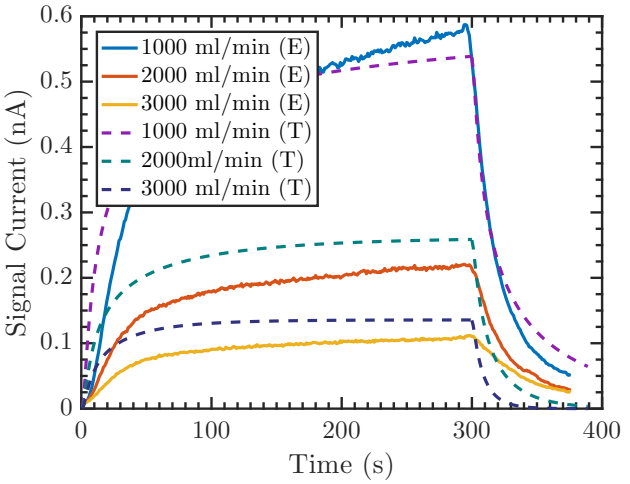

FIGURE 16: Three of the experimental results (Q = 1000 ml/min, 2000 ml/min and 3000 ml/min) compared to the theoretical model. (E) experimental results (T) Theoretical model (R^2_{1000} = 0.96, R^2_{2000} = 0.91, R^2_{3000} = 0.70)

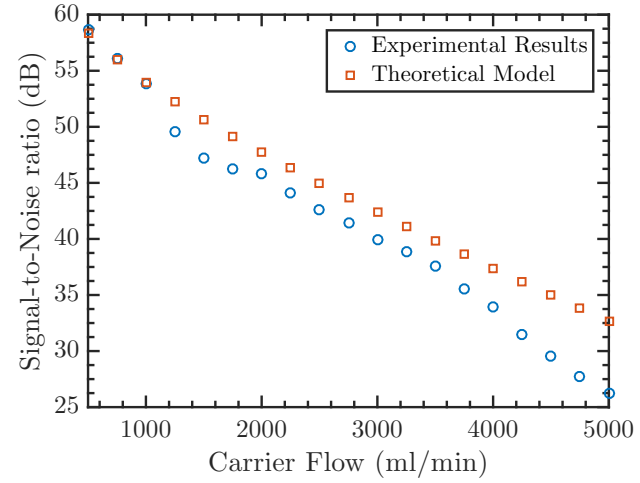

FIGURE 15: Experimental Results of the signal energy values obtained from the carrier flow (Q) study compared to the numerical results of the theoretical model (M = 0.8 ng, D = 0.35 cm^2/s, x = 2.5 cm, N = 2.8655e-4) (R^2 = 0.98)

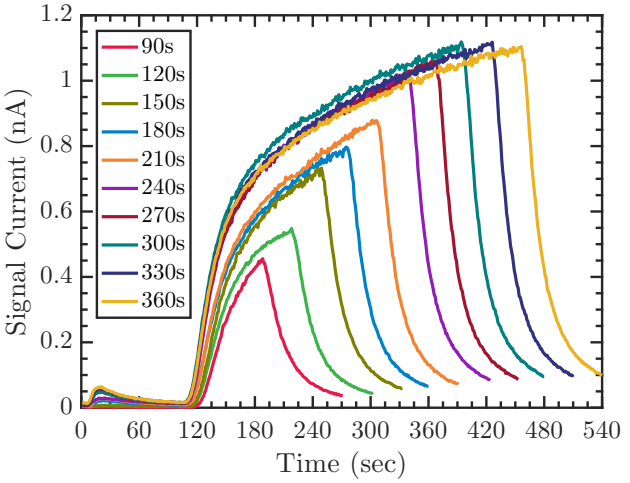

FIGURE 17: Experimental results of the pulse width experiment with pulse width varying from T = 90s to T = 360s with T = 30s increments

TABLE 3: Experimental Parameters for Bit Duration Experiment

Parameter	Symbol	Value	Unit
Tracked signal flow ion	m/z	43	Da
Signal flow	q	6	ml/min
Carrier flow	Q	1000	ml/min
Carrier flow pressure	P_F	1	bar
Transmission distance	x	2.5	cm
Diffusivity of acetone in air	D	0.124	cm^2/s

Table 3.

A. TRANSMITTED SIGNAL

The experimental result for the transmitted signal with varying length can be seen in Figure 17. It can be seen that as the bit duration (T) is increased the signal sees an increase in its amplitude and from Figure 19 sees an increase in the background noise (leftover from the bit transmission). However the rise of both the amplitude and the background signal decreases as bit length is increased. This behaviour is due to the detector reaching to the point where it absorbs all the chemicals in the bit transmission.

VII. CONCLUSION

In this paper, three main properties of macro-molecular communications are analyzed: signal flow (q) and carrier flow (Q) and the bit duration (T). Signal flow generates the signal used in transmission and the carrier flow aids in the transmission

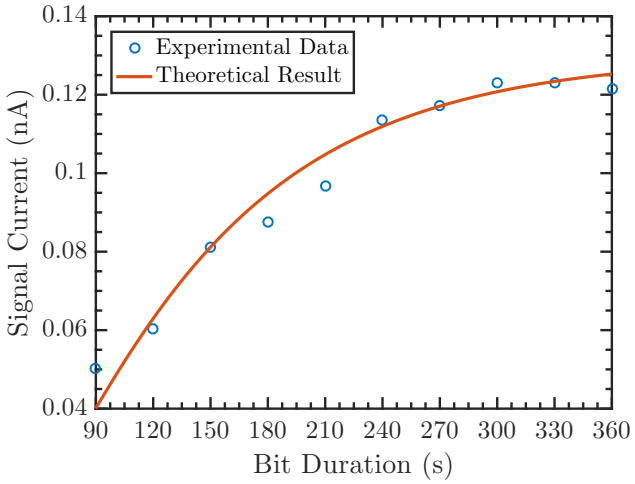

FIGURE 18: Experimental Result of the maximum signal current along with comparison the the theoretical model(M = 1.18 ng, D = 0.01 cm^2/s, x = 2.5 cm, u = 0.02 cm/s) (R^2 = 0.97)

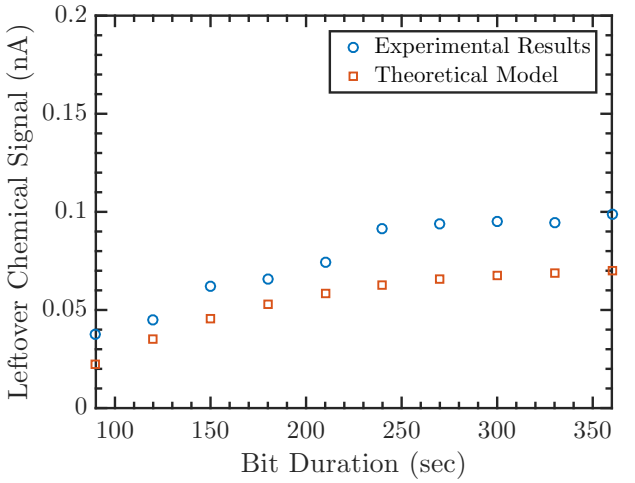

FIGURE 19: Experimental Result of the signal current generated from the leftover chemicals from the bit transmission with comparison the the theoretical model (M = 1.18 ng, D = 0.01 cm^2/s, x = 2.5 cm, u = 0.02 cm/s) (R^2 = 0.95)

by decreasing the time of response. To test these properties an experimental setup was utilized, consisting of a in-house built odor generator that generates the necessary pulses to create chemical messages and a quadrupole mass analyzer (QMA) with a membrane inlet to detect the transmitted chemical messages. Experiments on the signal analysis shows that the signal energy is quadratically dependent of the signal flow introduced into the system. Carrier flow (Q) behaves in a more complex way compared to the signal flow and has both advantages and disadvantages of using it. The presence of the carrier flow decreases the effect of the diffusive properties of the signal chemicals and make the signal behave similar to that of a square wave but the carrier flow diminishes the signal amplitude and therefore the energy, which can make the detection of the signal a challenge if the transmission is along

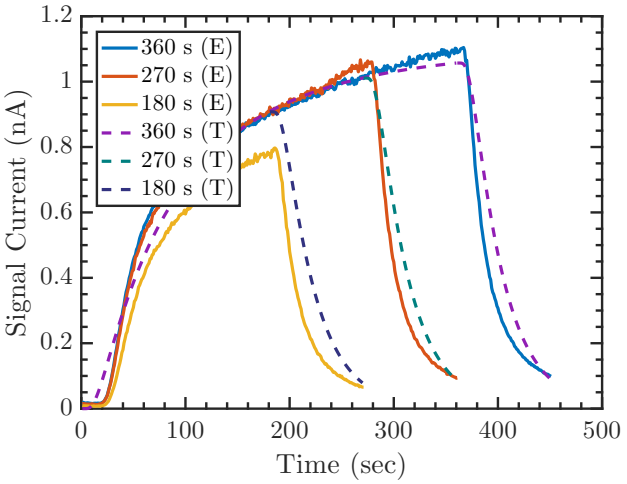

FIGURE 20: Three of the experimental results (T = 360 s, 270 s and 180 s) compared to the theoretical model. (E) experimental results (T) Theoretical model

a considerable distance. A final experiment was conducted to test the effects of bit duration of the communication system. The leftover chemicals from the transmission sees an increase as the bit duration is increased however, after a certain bit duration length, the system reaches a stable point which may be the effect of the membrane in the system.

A mathematical model for molecular communication is developed based on the absorbed chemicals in the transmission and based on the generalized form of the diffusion-advection equation. The model shows agreement with the experimental results by explaining the behaviour of the properties of the parameters studied in the paper. In future, the model will be developed further to explain the transmission of messages using molecular communications and the analytical calculations of Bit Error Rate (BER) with comparison to experimental data along with analysis of M-ary modulation will be studied.

APPENDIX

A. ABSORBED PARTICLES IN 2D AND 3D

Based on the solutions to the partial differential equation given in Eq. (6) and Eq. (7) the absorbed chemicals can be derived from the following equations.

$$\theta_c(x,y,t) = M - \int_{-y_\epsilon}^{y_d}\int_{-x_\epsilon}^{x_d} C(x,y,t)dxdy \tag{28}$$

$$\theta_c(x,y,z,t) = M - \int_{-z_\epsilon}^{z_d}\int_{-y_\epsilon}^{y_d}\int_{-x_\epsilon}^{x_d} C(x,y,z,t)dxdydz \tag{29}$$

Based on these equations the capture molecules in the system are as follows

$$\theta_c(x,y,t) = M - \frac{M}{4L_z}\left[\text{erf}\left(\frac{x_d - u_x t}{2\sqrt{D_x t}}\right) + \text{erf}\left(\frac{x_\epsilon + u_x t}{2\sqrt{D_x t}}\right)\right]\left[\text{erf}\left(\frac{y_d - u_y t}{2\sqrt{D_y t}}\right) + \text{erf}\left(\frac{y_\epsilon + u_y t}{2\sqrt{D_y t}}\right)\right] \quad (30)$$

$$\theta_c(x,y,z,t) = M - \frac{M}{8}\left[\text{erf}\left(\frac{x_d - u_x t}{2\sqrt{D_x t}}\right) + \text{erf}\left(\frac{x_\epsilon + u_x t}{2\sqrt{D_x t}}\right)\right]\left[\text{erf}\left(\frac{y - u_y t}{2\sqrt{D_y t}}\right) + \text{erf}\left(\frac{y_\epsilon + u_y t}{2\sqrt{D_y t}}\right)\right]\left[\text{erf}\left(\frac{z_d - u_z t}{2\sqrt{D_z t}}\right) + \text{erf}\left(\frac{z_\epsilon + u_z t}{2\sqrt{D_z t}}\right)\right] \quad (31)$$

ACKNOWLEDGMENT

The research was funded from the Engineering and Physical Sciences Research Council (EPSRC) under the grant agreement: EP/M029425/1 'Creating a Stink - Investigating Olfactory Transport Streams'.

REFERENCES

[1] R. Karban, I. T. Baldwin, K. J. Baxter, G. Laue, and G. Felton, "Communication between plants: induced resistance in wild tobacco plants following clipping of neighboring sagebrush," Oecologia, vol. 125, no. 1, pp. 66–71, 2000.

[2] T. D. Wyatt, Pheromones and animal behaviour: communication by smell and taste. Cambridge university press, 2003.

[3] B. D. Unluturk and I. F. Akyildiz, "An end-to-end model of plant pheromone channel for long range molecular communication," IEEE transactions on nanobioscience, vol. 16, no. 1, pp. 11–20, 2017.

[4] N. Vaughan, "Morphogenetic engineering for evolving ant colony pheromone communication," Proceedings of Artificial Intelligence and Simulation of Behaviour (AISB2018), 2018.

[5] S. Hiyama, Y. Moritani, T. Suda, R. Egashira, A. Enomoto, M. Moore, and T. Nakano, "Molecular communication," Journal-Institute of Electronics Information and Communication Engineers, vol. 89, no. 2, p. 162, 2006.

[6] N. Liley, "Chemical communication in fish," Canadian Journal of Fisheries and Aquatic Sciences, vol. 39, no. 1, pp. 22–35, 1982.

[7] W. C. Agosta, Chemical communication: the language of pheromones. Henry Holt and Company, 1992.

[8] T. Nakano, A. W. Eckford, and T. Haraguchi, Molecular communication. Cambridge University Press, 2013.

[9] I. F. Akyildiz, F. Brunetti, and C. Blázquez, "Nanonetworks: A new communication paradigm," Computer Networks, vol. 52, no. 12, pp. 2260–2279, 2008.

[10] N. Farsad, H. B. Yilmaz, A. Eckford, C.-B. Chae, and W. Guo, "A comprehensive survey of recent advancements in molecular communication," IEEE Communications Surveys & Tutorials, vol. 18, no. 3, pp. 1887–1919, 2016.

[11] B.-H. Koo, C. Lee, H. B. Yilmaz, N. Farsad, A. Eckford, and C.-B. Chae, "Molecular mimo: From theory to prototype," IEEE Journal on Selected Areas in Communications, vol. 34, no. 3, pp. 600–614, 2016.

[12] A. Ahmadzadeh, V. Jamali, A. Noel, and R. Schober, "Diffusive mobile molecular communications over time-variant channels," IEEE Communications Letters, vol. 21, no. 6, pp. 1265–1268, 2017.

[13] M. Pierobon, I. F. Akyildiz et al., "Diffusion-based noise analysis for molecular communication in nanonetworks," IEEE Transactions on Signal Processing, vol. 59, no. 6, pp. 2532–2547, 2011.

[14] I. Llatser, A. Cabellos-Aparicio, M. Pierobon, and E. Alarcón, "Detection techniques for diffusion-based molecular communication," IEEE Journal on Selected Areas in Communications, vol. 31, no. 12, pp. 726–734, 2013.

[15] A. Einolghozati, M. Sardari, and F. Fekri, "Capacity of diffusion-based molecular communication with ligand receptors," in Information Theory Workshop (ITW), 2011 IEEE. IEEE, 2011, pp. 85–89.

[16] S. Kadloor, R. S. Adve, and A. W. Eckford, "Molecular communication using brownian motion with drift," IEEE Transactions on NanoBioscience, vol. 11, no. 2, pp. 89–99, 2012.

[17] N.-R. Kim, A. W. Eckford, and C.-B. Chae, "Symbol interval optimization for molecular communication with drift," IEEE transactions on nanobioscience, vol. 13, no. 3, pp. 223–229, 2014.

[18] N. Tavakkoli, P. Azmi, and N. Mokari, "Performance evaluation and optimal detection of relay-assisted diffusion-based molecular communication with drift," IEEE Trans. Nanobiosci, vol. 16, no. 1, pp. 34–42, 2017.

[19] L. Lin, J. Zhang, M. Ma, and H. Yan, "Time synchronization for molecular communication with drift," IEEE Communications Letters, vol. 21, no. 3, pp. 476–479, 2017.

[20] N. Farsad, Y. Murin, A. Eckford, and A. Goldsmith, "On the capacity of diffusion-based molecular timing channels," in Information Theory (ISIT), 2016 IEEE International Symposium on. IEEE, 2016, pp. 1023–1027.

[21] M. Pierobon and I. F. Akyildiz, "Information capacity of diffusion-based molecular communication in nanonetworks," in INFOCOM, 2011 Proceedings IEEE. IEEE, 2011, pp. 506–510.

[22] D. Arifler, "Capacity analysis of a diffusion-based short-range molecular nano-communication channel," Computer Networks, vol. 55, no. 6, pp. 1426–1434, 2011.

[23] T. Nakano, Y. Okaie, and J.-Q. Liu, "Channel model and capacity analysis of molecular communication with brownian motion," IEEE communications letters, vol. 16, no. 6, pp. 797–800, 2012.

[24] M. Pierobon and I. F. Akyildiz, "Capacity of a diffusion-based molecular communication system with channel memory and molecular noise," IEEE Transactions on Information Theory, vol. 59, no. 2, pp. 942–954, 2013.

[25] N. Farsad, C. Rose, M. Médard, and A. Goldsmith, "Capacity of molecular channels with imperfect particle-intensity modulation and detection," in Information Theory (ISIT), 2017 IEEE International Symposium on. IEEE, 2017, pp. 2468–2472.

[26] N.-R. Kim and C.-B. Chae, "Novel modulation techniques using isomers as messenger molecules for nano communication networks via diffusion," IEEE Journal on Selected Areas in Communications, vol. 31, no. 12, pp. 847–856, 2013.

[27] M. S. Kuran, H. B. Yilmaz, T. Tugcu, and I. F. Akyildiz, "Modulation techniques for communication via diffusion in nanonetworks," in Communications (ICC), 2011 IEEE International Conference on. IEEE, 2011, pp. 1–5.

[28] H. Arjmandi, M. Movahednasab, A. Gohari, M. Mirmohseni, M. Nasiri-Kenari, and F. Fekri, "Isi-avoiding modulation for diffusion-based molecular communication," IEEE Transactions on Molecular, Biological and Multi-Scale Communications, vol. 3, no. 1, pp. 48–59, 2017.

[29] B. C. Akdeniz, A. E. Pusane, and T. Tugcu, "Position-based modulation in molecular communications," Nano communication networks, vol. 16, pp. 60–68, 2018.

[30] M. S. Leeson and M. D. Higgins, "Forward error correction for molecular communications," Nano Communication Networks, vol. 3, no. 3, pp. 161–167, 2012.

[31] M. Femminella, G. Reali, and A. V. Vasilakos, "A molecular communications model for drug delivery," IEEE transactions on nanobioscience, vol. 14, no. 8, pp. 935–945, 2015.

[32] T. Nakano, T. Suda, Y. Okaie, M. J. Moore, and A. V. Vasilakos, "Molecular communication among biological nanomachines: A layered architecture and research issues," IEEE transactions on nanobioscience, vol. 13, no. 3, pp. 169–197, 2014.

[33] M. Veletić, P. A. Floor, Z. Babić, and I. Balasingham, "Peer-to-peer communication in neuronal nano-network," IEEE Transactions on Communications, vol. 64, no. 3, pp. 1153–1166, 2016.

[34] L. P. Giné and I. F. Akyildiz, "Molecular communication options for long range nanonetworks," Computer Networks, vol. 53, no. 16, pp. 2753–2766, 2009.

[35] N. Farsad, W. Guo, and A. W. Eckford, "Tabletop molecular communication: Text messages through chemical signals," PloS one, vol. 8, no. 12, p. e82935, 2013.

[36] S. Giannoukos, D. Tunç McGuiness, A. Marshall, J. Smith, and S. Taylor, "A chemical alphabet for macromolecular communications." Analytical chemistry, 2018.

[37] S. Giannoukos, A. Marshall, S. Taylor, and J. Smith, "Molecular communication over gas stream channels using portable mass spectrometry,"

Journal of The American Society for Mass Spectrometry, vol. 28, no. 11, pp. 2371–2383, 2017.
[38] N. Farsad, D. Pan, and A. Goldsmith, "A novel experimental platform for in-vessel multi-chemical molecular communications," in GLOBECOM 2017-2017 IEEE Global Communications Conference. IEEE, 2017, pp. 1–6.
[39] H. Unterweger, J. Kirchner, W. Wicke, A. Ahmadzadeh, D. Ahmed, V. Jamali, C. Alexiou, G. Fischer, and R. Schober, "Experimental molecular communication testbed based on magnetic nanoparticles in duct flow," arXiv preprint arXiv:1803.06990, 2018.
[40] S. Wang, W. Guo, S. Qiu, and M. D. McDonnell, "Performance of macro-scale molecular communications with sensor cleanse time," in Telecommunications (ICT), 2014 21st International Conference on. IEEE, 2014, pp. 363–368.
[41] W. Guo, C. Mias, N. Farsad, and J.-L. Wu, "Molecular versus electromagnetic wave propagation loss in macro-scale environments," IEEE Transactions on Molecular, Biological and Multi-Scale Communications, vol. 1, no. 1, pp. 18–25, 2015.
[42] W. Guo, T. Asyhari, N. Farsad, H. B. Yilmaz, B. Li, A. Eckford, and C.-B. Chae, "Molecular communications: channel model and physical layer techniques," IEEE Wireless Communications, vol. 23, no. 4, pp. 120–127, 2016.
[43] F. Stajano, N. Hoult, I. Wassell, P. Bennett, C. Middleton, and K. Soga, "Smart bridges, smart tunnels: Transforming wireless sensor networks from research prototypes into robust engineering infrastructure," Ad Hoc Networks, vol. 8, no. 8, pp. 872–888, 2010.
[44] R. K. Vander Meer, M. D. Breed, K. E. Espelie, and M. L. Winston, "Pheromone communication in social insects," Ants, wasps, bees and termites. Westview, Boulder, CO, vol. 162, 1998.
[45] R. A. Russell, "An odour sensing robot draws inspiration from the insect world," in Bioelectromagnetism, 1998. Proceedings of the 2nd International Conference on. IEEE, 1998, pp. 49–50.
[46] Y. Kuwana, S. Nagasawa, I. Shimoyama, and R. Kanzaki, "Synthesis of the pheromone-oriented behaviour of silkworm moths by a mobile robot with moth antennae as pheromone sensors1," Biosensors and Bioelectronics, vol. 14, no. 2, pp. 195–202, 1999.
[47] R. C. Araneda, A. D. Kini, and S. Firestein, "The molecular receptive range of an odorant receptor," Nature neuroscience, vol. 3, no. 12, p. 1248, 2000.
[48] Y.-P. Hsieh, Y.-C. Lee, P.-J. Shih, P.-C. Yeh, and K.-C. Chen, "On the asynchronous information embedding for event-driven systems in molecular communications," Nano Communication Networks, vol. 4, no. 1, pp. 2–13, 2013.
[49] B. Krishnaswamy, C. M. Austin, J. P. Bardill, D. Russakow, G. L. Holst, B. K. Hammer, C. R. Forest, and R. Sivakumar, "Time-elapse communication: Bacterial communication on a microfluidic chip," IEEE Transactions on Communications, vol. 61, no. 12, pp. 5139–5151, 2013.
[50] M. Ş. Kuran, H. B. Yilmaz, T. Tugcu, and I. F. Akyildiz, "Interference effects on modulation techniques in diffusion based nanonetworks," Nano Communication Networks, vol. 3, no. 1, pp. 65–73, 2012.
[51] E. De Hoffmann and V. Stroobant, Mass spectrometry: principles and applications. John Wiley & Sons, 2007.
[52] S. Giannoukos, B. Brki?, S. Taylor, A. Marshall, and G. F. Verbeck, "Chemical sniffing instrumentation for security applications," Chemical reviews, vol. 116, no. 14, pp. 8146–8172, 2016.
[53] M. Statheropoulos, G. Pallis, K. Mikedi, S. Giannoukos, A. Agapiou, A. Pappa, A. Cole, W. Vautz, and C. P. Thomas, "Dynamic vapor generator that simulates transient odor emissions of victims entrapped in the voids of collapsed buildings," Analytical chemistry, vol. 86, no. 8, pp. 3887–3894, 2014.
[54] S. Giannoukos, B. Brki?, S. Taylor, and N. France, "Monitoring of human chemical signatures using membrane inlet mass spectrometry," Analytical chemistry, vol. 86, no. 2, pp. 1106–1114, 2013.
[55] B. Brkić, S. Giannoukos, N. France, R. Murcott, F. Siviero, and S. Taylor, "Optimized dlp linear ion trap for a portable non-scanning mass spectrometer," International Journal of Mass Spectrometry, vol. 369, pp. 30–35, 2014.
[56] S. Giannoukos, B. Brkić, and S. Taylor, "Analysis of chlorinated hydrocarbons in gas phase using a portable membrane inlet mass spectrometer," Analytical Methods, vol. 8, no. 36, pp. 6607–6615, 2016.
[57] S. Giannoukos, B. Brkić, S. Taylor, and N. France, "Membrane inlet mass spectrometry for homeland security and forensic applications," Journal of the American Society for Mass Spectrometry, vol. 26, no. 2, pp. 231–239, 2015.
[58] S. Giannoukos, A. Agapiou, and S. Taylor, "Advances in chemical sensing technologies for vocs in breath for security/threat assessment, illicit drug detection, and human trafficking activity," Journal of breath research, vol. 12, no. 2, p. 027106, 2018.
[59] S. Giannoukos, M. J. A. Joseph, and S. Taylor, "Portable mass spectrometry for the direct analysis and quantification of volatile halogenated hydrocarbons in the gas phase," Analytical Methods, vol. 9, no. 6, pp. 910–920, 2017.
[60] J. Crank, The mathematics of diffusion. Oxford university press, 1979.
[61] C. E. Baukal Jr, V. Gershtein, and X. J. Li, Computational fluid dynamics in industrial combustion. CRC press, 2000.